# Single-particle spectral function of the Holstein-Hubbard bipolaron

Martin Hohenadler,* Markus Aichhorn, and Wolfgang von der Linden
*Institute for Theoretical and Computational Physics, Graz University of Technology, Petersgasse 16, 8010 Graz, Austria*
(Received 25 May 2004; revised manuscript received 5 October 2004; published 14 January 2005)

The one-electron spectral function of the Holstein-Hubbard bipolaron in one dimension is studied using cluster perturbation theory together with the Lanczos method. In contrast to other approaches, this allows one to calculate the spectrum at continuous wave vectors and thereby to investigate the dispersion and the spectral weight of quasiparticle features. The formation of polarons and bipolarons, and their manifestation in the spectral properties of the system, is studied for the cases of intermediate and large phonon frequencies, with and without Coulomb repulsion. A good agreement is found with the most accurate calculations of the bipolaron band dispersion available. Pronounced deviations of the bipolaron band structure from a simple tight-binding band are observed, which can be attributed to next-nearest-neighbor hopping processes.

DOI: 10.1103/PhysRevB.71.014302 PACS number(s): 63.20.Kr, 71.27.+a, 71.38.Mx

## I. INTRODUCTION

In recent years, angle-resolved photoemission spectroscopy (ARPES) has proved to be very helpful in obtaining information about the electronic states of strongly correlated systems. While a lot of data is available from experiments, reliable theoretical calculations of the one-particle spectral function—which can often be regarded as being proportional to the ARPES spectrum—for popular models of, e.g., the Hubbard or *t-J* type, are usually very demanding. As a consequence, many interesting problems of condensed matter physics have not been investigated systematically regarding their spectral properties in a satisfactory way. Among them is the *bipolaron problem* of two electrons, which can form a bound state even in the presence of strong Coulomb repulsion if they are coupled to phonons. Despite the long history of this problem, bipolaron formation is still the subject of ongoing discussion due to its potential role, e.g., in high-temperature superconductors[1] and manganites,[2] two classes of materials studied extensively over the past decade.

Most existing results for the Holstein-Hubbard (HH) model considered here have been obtained using exact diagonalization (ED). Apart from a systematic error due to the necessary truncation of the Hilbert space, this method gives exact results for the one-electron spectrum, but is restricted to rather small systems, especially for small phonon frequencies and/or strong electron-phonon coupling. Consequently, it is difficult to study the dispersion of the spectral peaks throughout the Brillouin zone. To overcome this limitation, we employ here cluster perturbation theory (CPT), extending the recent application to the Holstein model with one electron.[3] In contrast to ED, CPT permits one to calculate the spectral function for continuous wave vectors. Moreover, finite-size effects are strongly reduced compared to direct diagonalization of small clusters, and results are much more realistic than previous work based on, e.g., a two-site system.[4–6] CPT becomes exact in the weak- and strong-coupling regimes, and has been successfully applied also to other problems.[7–14] A review of cluster methods for strongly correlated systems is by Maier *et al.*[15] Here we would merely like to point out the recent application of the dynamical cluster approximation to the half-filled Holstein model by Hague.[16]

In this work, we study in detail the formation of polarons and bipolarons, and its dependence on phonon frequency and electron-phonon and electron-electron interaction. To test the reliability of our results, and to interpret the quasiparticle (QP) features in the spectra, comparison is made to ED, as well as to the most accurate approach to the one-dimensional HH bipolaron currently available, namely, the variational diagonalization method.[17] Moreover, we also investigate the form of the bipolaron band dispersion and compare it to that of models with nearest-neighbor and next-nearest-neighbor hopping.

This paper is organized as follows. We begin with a review of the HH bipolaron in Sec. II. In Sec. III, we discuss some details of the application of CPT. Results are presented in Sec. IV and, finally, Sec. V contains our conclusions.

## II. THE HOLSTEIN-HUBBARD MODEL

The HH model is defined by the Hamiltonian

$$H = -t\sum_{\langle ij\rangle\sigma}\left(c_{i\sigma}^{\dagger}c_{j\sigma}+\text{H.c.}\right)+\omega\sum_{i}b_{i}^{\dagger}b_{i}-g\sum_{i}n_{i}(b_{i}^{\dagger}+b_{i}) + U\sum_{i}n_{i\uparrow}n_{i\downarrow}. \quad (1)$$

Here $c_{i\sigma}^{\dagger}$ ($c_{i\sigma}$) and $b_{i}^{\dagger}$ ($b_{i}$) create (annihilate) an electron of spin $\sigma$ and a phonon of energy $\omega$ ($\hbar=1$) at site $i$, respectively, and $n_i=\Sigma_\sigma n_{i\sigma}$ with $n_{i\sigma}=c_{i\sigma}^{\dagger}c_{i\sigma}$. The first two terms correspond to the kinetic energy of the electrons and the kinetic and elastic energy of the phonons, respectively. The electron-phonon (el-ph) and electron-electron (el-el) interactions are described by the third and fourth terms. We have three model parameters, namely, the amplitude for nearest-neighbor hopping, $t$, the phonon frequency $\omega$, the el-ph coupling constant $g$, and the el-el interaction strength $U>0$. For $U=0$, Eq. (1) is identical to the pure Holstein model, while for $g=0$ we recover the Hubbard model. We introduce the commonly used dimensionless coupling constant $\lambda=2g^2/(\omega W)$, where $W=4tD$ is the bare bandwidth in $D$ dimensions. We further define the dimensionless parameters $\bar{\omega}=\omega/t$ and $\bar{U}=U/t$, and express all energies in units of $t$.

 

Consequently, the independent parameters of the model are $\bar{\omega}$, $\bar{U}$, and $\lambda$. In the following, we shall also use the polaron binding energy $E_P=\lambda W/2$, which emerges as a natural parameter from the Lang-Firsov transformation.[18] Finally, the lattice constant is taken to be unity.

Owing to the complexity of even the two-electron problem, we will not discuss effects of bipolaron-bipolaron interaction here. An investigation of the latter, which will definitely play an important role in real materials, requires a study of the HH model with many electrons (see, e.g., Ref. 19 and references therein), which is beyond the scope of our method in its present form.

There exists a considerable amount of work on the HH bipolaron, although it is by far not as well understood as the simpler one-electron case. In the following, we restrict our discussion to recent developments in the field. A very complete review of earlier work has been given by Alexandrov and Mott.[20]

While the pairing of electrons in momentum space can be accurately described by Migdal-Eliashberg theory[21] for weak enough coupling, no reliable theory is available for the formation of bipolarons—corresponding to pairing of electrons in real space—at intermediate to strong el-ph interaction. In recent years, progress was made using either variational approaches[22–28] or, more importantly, unbiased numerical studies based on ED,[4–6,29,30] variational diagonalization,[17,31–33] density matrix renormalization group (DMRG),[34] and quantum Monte Carlo (QMC) methods.[35–37] The ED and DMRG calculations were restricted to rather small systems consisting of two,[4–6] four,[29] six,[34] eight,[30,31] or twelve sites,[32] while the methods of Refs. 17, 35, and 36 are almost free of finite-size effects. The larger number of phonon states required to obtain converged results makes numerical studies with ED methods even more challenging than for a single electron, especially for small phonon frequencies.

Since the HH model represents a simplified description of the situation in real materials, it is highly desirable to study more complex models. To this end, it is interesting to note that the QMC methods of de Raedt and Lagendijk[35] and Macridin *et al.*[36] may be generalized to include dispersive phonons. Furthermore, both approaches can be applied to models with long-range Coulomb interaction,[35,36] similar to the work of Bonča and Trugman.[38] Finally, bipolaron formation in a model with Jahn-Teller modes—as present, e.g., in perovskite manganites—has recently been investigated by Shawish *et al.*[33]

To discuss bipolaron formation in the HH model, we have to distinguish between two cases. The two electrons can have either the same or opposite spin, which leads to a singlet or triplet state, respectively. We consider these possibilities separately.

### A. Singlet state

For two electrons in a singlet state, the formation of a bound bipolaron state in the absence of Coulomb interaction originates from the fact that the potential well—arising from a displacement of the oscillators—around an occupied lattice site deepens in the presence of a second electron. This may easily be seen in the atomic limit $t=0$, using the Lang-Firsov transformation.[18] On different lattice sites, each electron gains an energy $-E_P$ by distorting the lattice, whereas the energy shift becomes $-4E_P$ if both particles occupy the same site (*small or on-site bipolaron*). For $t\neq 0$, the competition between the kinetic energy of the electrons on the one hand and the displacement or lattice energy on the other hand determines the cross over from a state with two weakly bound polarons, sometimes also referred to as a *large bipolaron*, for $\lambda<\lambda_c$ to a small bipolaron for $\lambda>\lambda_c$, where $\lambda_c$ denotes the critical value of the el-ph coupling. In Sec. II, $\lambda$ has been defined as $\lambda=2E_P/W$, i.e., as the ratio of the energy gain due to polaron formation to the kinetic energy of a free electron. While $\lambda_c=1$ in the adiabatic regime for the small-polaron crossover in the model with one electron (see, e.g., discussion in Ref. 39), here we expect $\lambda_c=0.5$ (for $\bar{\omega}\ll 1$) due to the energy gain of $-2E_P$ per electron compared to $-E_P$ in the single-polaron problem. This is well confirmed by the calculations of Wellein *et al.*,[30] who find a strong decrease of the kinetic energy near $\lambda=0.5$ for $\bar{\omega}=0.4$.

For $\bar{\omega}\gg 1$, the lattice energy becomes important since the trapping of the carriers requires a sizable lattice distortion. This gives rise to the additional condition $2\sqrt{E_P/\omega}>1$ for a small bipolaron.[40] Similar to the one-electron problem, the crossover is very gradual in the nonadiabatic regime.[30] The correlation or binding of the two electrons depends crucially on the phonon frequency, since the latter determines the maximum distance across which the two particles feel an attractive interaction due to the phonons. Up to second order in $g$, this coupling is given by

$$U_{\mathrm{eff}}(\epsilon)=g^2\mathcal{D}_{\mathrm{ph}}(\boldsymbol{q},\epsilon)=-\frac{2g^2\omega}{\omega^2-\epsilon^2}, \tag{2}$$

where $\mathcal{D}_{\mathrm{ph}}(\boldsymbol{q},\epsilon)$ denotes the phonon propagator. Equation (2) reveals that the energy-dependent interaction is attractive for $\epsilon<\omega$, and becomes instantaneous in the antiadiabatic limit $\omega\to\infty$ where $U_{\mathrm{eff}}=-2g^2/\omega$. Hence, the binding always decreases with increasing phonon frequency.[29]

For $U>0$, there is a competition between the retarded, attractive interaction mediated by the phonons and the instantaneous, repulsive Hubbard interaction. Consequently, a state with two unbound polarons—stabilized by the onsite repulsion—can exist for sufficiently weak el-ph coupling.[30] This is in contrast to the extended HH model with long-range interaction, in which a bipolaron state is formed irrespective of the value of $U$.[41] The effective el-el interaction in the HH model determining the nature of the bipolaron state is

$$U_{\mathrm{eff}}=U-2E_P. \tag{3}$$

From this result, which can be obtained either from the generalization of Eq. (2) to $U\neq 0$ in the limit $\omega\to\infty$, or in the antiadiabatic strong-coupling limit,[36] one may be tempted to expect a bipolaron state to exist only for $U_{\mathrm{eff}}<0$, i.e., if there is a net attractive interaction between the particles. While this is true for the effective Hubbard model onto which the HH model maps in the antiadiabatic strong-coupling limit, a consideration of virtual hopping processes leads to the less

stringent condition $U<4E_{\mathrm{P}}$.[17] The energy gain due to virtual exchange processes of two electrons on neighboring lattice sites—not suppressed by strong el-ph coupling—permits the formation of a weakly bound *intersite bipolaron* with the two electrons most likely to reside on neighboring lattice sites.[17,36] A phase diagram for bipolaron formation as a function of $\lambda$ and $\overline{\omega}$ in one dimension has been presented by Weiße *et al.*[32] Eventually, for sufficiently strong el-ph coupling $2E_{\mathrm{P}}\gtrsim U$, the effective on-site potential $U_{\mathrm{eff}}$ becomes attractive, and a small bipolaron is formed.

Starting from a small bipolaron, a crossover to an intersite bipolaron takes place when the Coulomb interaction becomes large enough.[17,36,41] The intersite bipolaron has a much smaller effective mass than the small bipolaron and may therefore also exist as a mobile carrier in real materials.[17] In the adiabatic limit $\overline{\omega}=0$, the on-site-intersite bipolaron transition has been shown to be of first order,[25,26] but for finite phonon frequencies it is expected to happen in a more gradual way because of retardation effects, in agreement with recent calculations.[17] Estimates for the region of existence of the intersite bipolaron state for $\overline{\omega}=1$ are $U<2E_{\mathrm{P}}$ for weak coupling, and $U<4E_{\mathrm{P}}$ for strong el-ph coupling,[17] and phase diagrams in the $(U,\lambda)$ plane have been reported in one[17] and two dimensions.[36] While the above conditions are quite accurate in the nonadiabatic regime $\overline{\omega}\geqslant 1$, the case $\overline{\omega}\ll 1$ remains an open problem.

Finally, the physically most interesting regime, which is unfortunately also the most difficult case to treat theoretically, is defined by $\overline{\omega}\ll 1$, and a Coulomb repulsion at least as large as the attractive interaction due to the el-ph coupling.

### B. Triplet state

For two electrons of the same spin, the Pauli principle forbids double occupation of a site. In principle, a bound state may be formed with the two particles being located on different lattice sites. While two electrons can lower their energy by sharing a lattice distortion in the large-bipolaron regime, especially for small phonon frequencies, the exchange process stabilizing the singlet intersite bipolaron state at intermediate-to-strong el-ph coupling and $U>0$ is not strong enough to bind two polarons in a triplet intersite state.[17] Furthermore, for $U<\infty$, the ground-state energy of the triplet state is always larger than for a singlet state because two particles with parallel spin cannot occupy the same $\boldsymbol{k}=\mathbf{0}$ energy level. Finally, the singlet and triplet states become degenerate in the limit $U\rightarrow\infty$.

## III. METHOD

As mentioned above, here we use CPT in combination with the Lanczos recursion method.[42] Details about the application to el-ph problems have been given in Ref. 3, henceforth also referred to as I. The major difficulty we are facing in the present case is the larger number of phonon states needed to obtain converged results. From a physical point of view, this is not surprising since each of the two electrons will create a lattice distortion or phonon cloud, whereas there is only one dressed particle (polaron) in the case of the Holstein polaron considered in I. However, in addition to the simple doubling of the number of particles, it has been shown by previous authors[29,30,34] that multiphonon states play a more important role for the bipolaron as a result of the phonon-mediated binding.

ED (and also CPT) for el-ph systems is affected both by finite-size effects and the truncation error due to the restricted number of phonon states kept in calculations. Obviously, if one used very small clusters, good convergence with respect to the phonons could be achieved even for strong el-ph coupling. On the other hand, for small numbers of phonon states, rather large clusters can be studied. The approach which has been widely used in the past is to require the truncation error, e.g., of the ground-state energy, to be smaller than a certain limit, and to use the maximal cluster size which can be handled for this number of phonons. Here, an additional challenge arises form the fact that the diagonalization of the cluster has to be performed for open boundary conditions.[3] Consequently, one cannot exploit translational symmetry to reduce the dimensionality of the Hilbert space. However, this drawback is clearly outweighed by the advantages of CPT outlined below.

We would like to briefly discuss some interesting features of CPT. The method is based on a breakup of the infinite lattice into clusters of $N$ sites, say.[8] The one-electron cluster Green function, denoted here as $G_{ab,\sigma}$ [see Eq. (4) in I], of the model under consideration is calculated for one of these (identical) clusters using open boundary conditions. This can be done, e.g., using ED or analytical approaches.[3] The hopping between adjacent clusters is then treated as a perturbation to obtain the Green function of the original system, $\mathcal{G}_{\sigma}(\boldsymbol{k},\epsilon)$.[8] A basic limitation of the theory is that the Hamiltonian must not contain any nonlocal interactions, except for one-electron terms. Additionally, CPT in its present form can only be used to calculate one-particle Green functions.[8] Therefore, interesting observables such as, e.g., el-el correlation functions or transport properties are not yet available.

From the nature of the approximation made, it is clear that CPT will work particularly well if the local interactions dominate the physics of the system, i.e., for the case of the HH model (1), if $g$, $U\gg t$. This point will be illustrated in Sec. IV. The method becomes exact in the atomic limit $t=0$, for noninteracting electrons ($g$, $U=0$), as well as for $N=\infty$.[8] The quality of the results obtained with CPT has been tested for several models,[7–14] and a very good agreement with other work has been found. In I, we pointed out the occurrence of finite-size effects which show up as additional peaks in the corresponding one-electron spectral function. The weight of the latter reduces quickly as $N\rightarrow\infty$, so that the spectrum is not affected significantly.

One of the most important advantages of CPT is that it gives, in principle, results for an infinite system, although the approximate treatment of the intercluster hopping introduces some finite-size effects, which can be systematically reduced by increasing the cluster size. As a consequence, the one-electron Green function can be calculated for any wave vector in the Brillouin zone, even for $N=1$. This allows one to study the dispersion of the QP peaks, in strong contrast to standard ED methods on finite clusters, for which only a few

points in momentum space are accessible, owing to the rather small values of $N \approx 2$–$20$ usually used.

Since we consider only the one-dimensional HH model in the following, we shall adopt the notation accordingly. We are interested in the one-electron Green function

$$\mathcal{G}_\sigma(k,\epsilon) = \langle\downarrow| c_{k\sigma} \frac{1}{\epsilon - H} c_{k\sigma}^\dagger |\downarrow\rangle, \tag{4}$$

where $|\downarrow\rangle$ denotes the ground state with one electron of spin down, and $\sigma = \uparrow, \downarrow$. Equation (4) contains only the inverse photoemission part of the total one-electron Green function. In the case of $\mathcal{G}_\uparrow$, the second part—corresponding to photoemission—vanishes, since there is no $\uparrow$ electron in the ground state. The situation would be different if we started with a two-electron (singlet or triplet) ground state. Then, the photoemission part of the one-electron spectral function also contains valuable information. However, due to limited computer memory, such computations involving three-electron states are not possible with the code used here.

In Eq. (4), we have omitted the energy $E_0^\downarrow$ of the ground state $|\downarrow\rangle$, which usually enters in the form $H - E_0^\downarrow$, to permit direct comparison with the singlet bipolaron band dispersion $E^{\uparrow\downarrow}(k)$ in Sec. IV. The one-electron spectral function is related to the Green function (4) via

$$A_\sigma(k,\epsilon) = -\pi^{-1} \lim_{\eta \to 0^+} \mathrm{Im}\, \mathcal{G}_\sigma(k, \epsilon + i\eta). \tag{5}$$

To calculate the cluster Green function by ED, a truncation of the phonon Hilbert space is necessary, and we use the same truncation scheme as in I. The number of phonon states $N_{\mathrm{ph}}$ will be chosen so as to push the truncation error $\Delta \equiv |E_0^{\uparrow\downarrow}(N_{\mathrm{ph}}+1) - E_0^{\uparrow\downarrow}(N_{\mathrm{ph}})| / |E_0^{\uparrow\downarrow}(N_{\mathrm{ph}})|$ of the energy $E_0^{\uparrow\downarrow}$ of the two-electron ground state $|\uparrow\downarrow\rangle$ below $10^{-4}$. The use of $E_0^{\uparrow\downarrow}$ to monitor convergence with respect to $N_{\mathrm{ph}}$ comes from the observation that—for the same number of phonons—the truncation error of the latter is always smaller than for the triplet state $|\downarrow\downarrow\rangle$. This may be ascribed to the fact that for two electrons of the same spin, no bound on-site or intersite state exists. In particular, there will be no large local lattice distortion surrounding an onsite bipolaron, the description of which requires a significant number of phonons. In previous work on the HH bipolaron, using ED with periodic boundary conditions,[4–6,29,30] the truncation error was usually smaller than $10^{-6}$. However, these methods were restricted to only a few $k$ vectors. Furthermore, our calculations show that even a relative error $\Delta = 10^{-4}$ ensures satisfactory convergence of the one-electron spectrum. The smaller number of phonon states enables us to use larger clusters and thereby significantly diminish finite-size effects since, within the CPT, even an increase $N \to N+1$ noticeably improves the results. Once the cluster size has been fixed, we use the maximal possible number of phonons. The accuracy $\Delta$ varies for the different calculations and will be reported in each figure.

In its present form, our method is restricted to the nonadiabatic regime $\overline{\omega} \geqslant 1$, except for weak el-ph coupling. To study smaller phonon frequencies—relevant to, e.g., transition metal oxides—a combination with variational diagonalization techniques or the use of shared-memory systems would be necessary. As in I, we restrict our calculations to the spectral function, which is the most fundamental quantity that can be obtained from CPT.[8]

## IV. RESULTS

The one-electron spectral function of the problem considered here has been calculated before using ED (Refs. 4–6) and DMRG,[34] both in one dimension. However, results were given only for $k=0$, and for very small systems with $N=2$ and 6, respectively. With the above methods, and for periodic boundary conditions, the spectral function (5) can be evaluated for $N$ different wave vectors, of which only $N/2+1$ are physically nonequivalent. This makes it difficult or even impossible to study the dispersion of QP features. Recently, a parallelized DMRG code has been developed,[43] which allows studies of one-dimensional Holstein models on very large clusters even at half filling.[19] However, the calculation of spectral functions within DMRG is very time consuming, since it has to be done separately for each point on the energy axis. Several authors have also calculated dressed spectral functions,[5,6,34] with the fermion operators in Eq. (4) replaced by their Lang-Firsov transformed (i.e., dressed) counterparts, as well as pair spectral functions.[34] The corresponding spectra show a simplified structure in certain regimes, indicating that polarons and bipolarons are "good" QP's for these parameters.

De Mello and Ranninger[5] have pointed out that to study the crossover between polarons and bipolarons it is, in general, necessary to investigate both photoemission and inverse photoemission. This can easily be understood by considering electron emission from the two-electron singlet ground state, i.e., the Green function $\langle\uparrow\downarrow| c_{k\uparrow}^\dagger (\epsilon - H)^{-1} c_{k\uparrow} |\uparrow\downarrow\rangle$. Depending on the parameters, $|\uparrow\downarrow\rangle$ may consist of either two weakly bound polarons or a bipolaron. Consequently, photoemission spectra will show only a single QP band. In contrast, the Green function (4) with $\sigma = \uparrow$ corresponds to adding an $\uparrow$ electron to the one-electron ground state $|\downarrow\rangle$. For example, the additional particle can either go into the ground state to form a bipolaron, or go into an excited polaron state. In general, we therefore expect two QP bands in the spectral function, whose weights, positions, and widths vary with $\overline{\omega}$, $\overline{U}$, and $\lambda$.

As we will compare our findings with the variational diagonalization method (VDM) of Bonča *et al.*,[17,33] we would like to comment on the accuracy of the latter. The problem is defined on an infinite system, so that the approach is free of boundary finite-size effects. However, the method involves a variationally determined Hilbert space with two variational parameters, namely, the maximal allowed distance between electrons and phonons, and between the two electrons, respectively. For the bipolaron problem under consideration, the limiting parameter in the regime $\overline{\omega} \geqslant 1$ is the maximum distance $N_{\mathrm{h}}$ between the two electrons. The results presented here have been obtained using $N_{\mathrm{h}} \leqslant 18$. While the method gives very accurate results—with errors smaller than the linewidth in the figures—for the case of a small bipolaron ($U \ll 2E_{\mathrm{P}}$), it is less reliable (relative errors $\lesssim 1\%$) for strong on-site repulsion $U \gg 2E_{\mathrm{P}}$ favoring two weakly bound polarons, similar to ED and CPT. Due to additional towers of

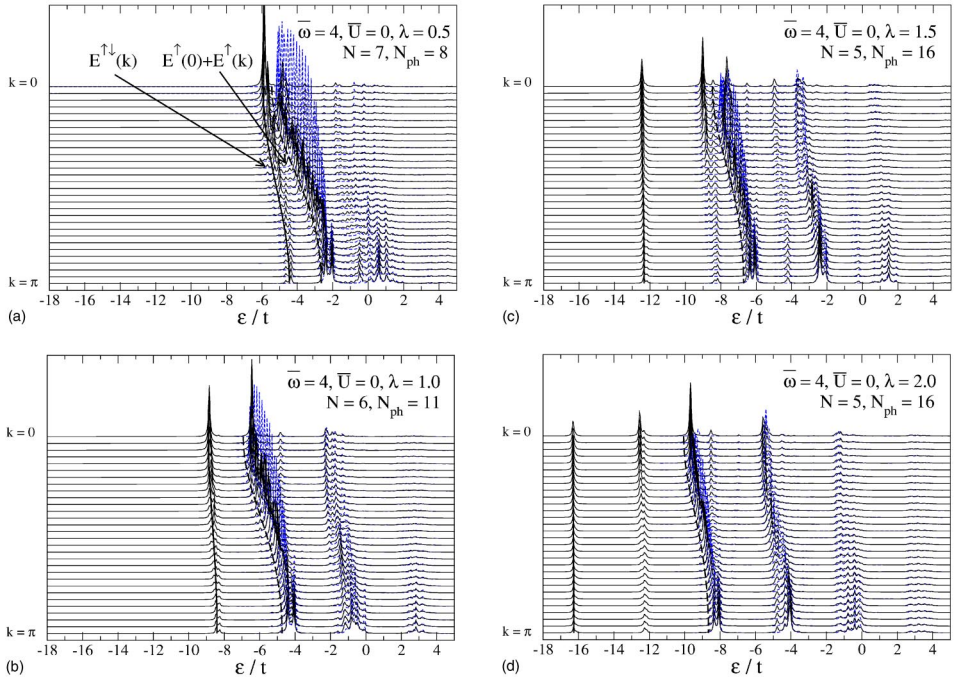


FIG. 1. (Color online) Spectral functions $A_\uparrow(k,\epsilon)$ (solid lines) and $A_\downarrow(k,\epsilon)$ (dashed lines) calculated with CPT for different values of the el-ph coupling λ, using $\eta=0.05t$ [see Eq. (5)]. All other parameters as indicated in the figures. The truncation errors are $\Delta<$ (a) $5.3\times10^{-6}$, (b) $1.0\times10^{-5}$, (c) $2.4\times10^{-7}$, (d) $6.7\times10^{-6}$ (see text). The vertical lines correspond to VDM results for the polaron and bipolaron band dispersions $E^\uparrow(0)+E^\uparrow(k)$ (dashed) and $E^{\uparrow\downarrow}(k)$ (solid), respectively (Ref. 44).

phonon excitations that are located in the neighborhood of the electron sites, the method achieves good convergence in the small-bipolaron regime even for strong coupling. Nevertheless, the adiabatic regime $\bar{\omega}\ll1$ represents a difficult problem, as is the case for other approaches. Finally, as in CPT, results may be obtained at any wave vector.

We shall see below that there is a close correspondence of the QP bands in the spectra to the polaron and bipolaron dispersion relations denoted here as $E^\uparrow(k)$ and $E^{\uparrow\downarrow}(k)$, respectively. The notation $E^\uparrow(k)$ is convenient, but there is no spin dependence in the case of a single electron, i.e., $E^\uparrow(k)=E^\downarrow(k)$. Results for $E^{\uparrow\downarrow}(k)$ have been reported by Wellein *et al.*[30] and Weiße *et al.*[32,41] However, in contrast to $A_\sigma(k,\epsilon)$, $E^\uparrow(k)$ and $E^{\uparrow\downarrow}(k)$ do not reveal the spectral weight of the corresponding QP's. Nevertheless, the comparison with the spectra will yield valuable insight and serve as a test of the CPT results. Moreover, a direct calculation of energy bands does not suffer from the restricted energy resolution of CPT due to the use of a smearing parameter [Eq. (5)].

Owing to the limitations regarding the number of phonon states, we shall show only results for $\bar{\omega}\geqslant1$. To be more specific, we consider two values of the adiabatic ratio, namely, $\bar{\omega}=4$ and 1. For $\bar{\omega}=4$, the spectra will turn out to be relatively simple, and we are able to study even strong el-ph coupling. Consequently, we start with a discussion of the antiadiabatic regime, and then move on to the more difficult case $\bar{\omega}=1$.

### A. Antiadiabatic regime

In this section, we restrict the discussion to $\bar{U}=0$, while the influence of Coulomb repulsion will be studied below. Figure 1 shows the evolution of the one-particle spectrum with increasing el-ph coupling. Here and in subsequent figures, solid lines represent results for $A_\uparrow$ and dashed lines correspond to $A_\downarrow$.

For $U=0$, two electrons of opposite spin always form a bipolaron state for any $\lambda>0$. At weak coupling $\lambda=0.5$ [Fig. 1(a)], $A_\uparrow$ exhibits two well visible bands, as well as an incoherent part centered at $\epsilon\approx0$. To understand the nature of the coherent excitations, we have also included in Fig. 1 the bipolaron band dispersion $E^{\uparrow\downarrow}(k)$ (solid vertical line), calculated by the VDM.[44] The latter fits well the low-energy band, with the minor deviations at intermediate $k$—i.e., the splitting of the low-energy peak into several small satellites—being finite-size effects, as has been verified by calculations on smaller and larger clusters for a smaller number of phonon states (not shown). A more detailed discussion of finite-size effects will be given below for $\bar{\omega}=1$.

Even at weak coupling $\lambda=0.5$, the bipolaron band already has a relatively small width of $W'/W\approx0.37$ compared to the free-electron value $W$. Moreover, the spectral weight of the lowest-energy peak, obtained by integration over the CPT spectrum, decreases significantly from about 0.68 at $k=0$ to about 0.08 at $k=\pi$. At the same time, the weight contained in the incoherent part of the spectrum increases with increasing $k$. This behavior is very similar to the single-electron case.[3]

We now turn our attention to the second, higher-lying band appearing in Fig. 1(a). From the general discussion in Sec. II, we expect that it corresponds to an excited state with two polarons. We therefore compare it to the energy of two independent polarons in an infinite system. Since $A_\uparrow$ describes the process of adding an electron with momentum $k$ to the one-polaron ground state with energy $E^\uparrow(0)$ [cf. Eq.

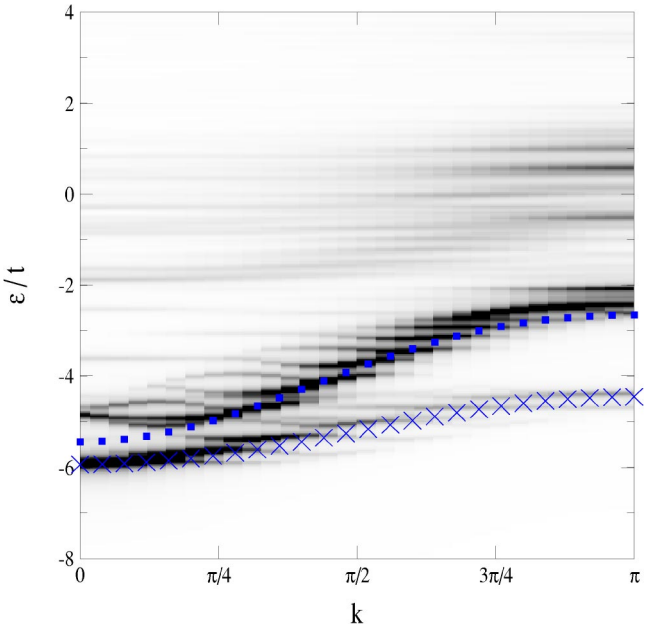


FIG. 2. (Color online) Density plot of the spectral function $A_{\uparrow}(k,\epsilon)$ for $\overline{\omega}=4.0$, $\overline{U}=0$, and $\lambda=0.5$, as shown in Fig. 1(a). The symbols correspond to VDM results for $E^{\uparrow}(0)+E^{\uparrow}(k)$ (squares) and $E^{\uparrow\downarrow}(k)$ (crosses), respectively (Ref. 44).

(4)], we show in Fig. 1(a) the band dispersion $E^{\uparrow}(0)+E^{\uparrow}(k)$ (dashed vertical line). The comparison with the spectral function yields a very good agreement at intermediate and large $k$, while there are some discrepancies at small momenta. A density plot of $A_{\uparrow}$ (Fig. 2) reveals more clearly that the two coherent bands hybridize and repel each other near the point where they would be degenerate, giving rise to an upper band with inversed dispersion at small $k$. The situation is similar to the hybridization of the coherent and incoherent parts in the one-electron case occurring for $|E^{\uparrow}(k)-E^{\uparrow}(0)| \sim \overline{\omega}$ (see I). Of course, such effects are absent in the band dispersion of a system with two independent polarons. Since the residual interaction between two polarons vanishes in the limit $N\rightarrow\infty$, the hybridization visible in the CPT spectrum may be attributed to finite-size effects. The latter originate from the fact that within CPT, translational symmetry is broken by treating inter- and intracluster hopping differently, and only approximately restored afterward.

The spectral function $A_{\downarrow}$, also shown in Fig. 1(a), contains a coherent band at low energies, and an incoherent part which is very similar to that of $A_{\uparrow}$. Well away from $k=0$, the coherent peaks in $A_{\downarrow}$ follow closely the polaron band in $A_{\uparrow}$. Thus the excited two-polaron state of the system with two electrons of opposite spin is very similar to the ground state of the system with two electrons of the same spin. Near $k=0$, the spectral weight of the low-energy peak in $A_{\downarrow}$ is small ($\approx 0.08$) compared to the polaron peak in $A_{\uparrow}$($\approx 0.2$). This is a result of the fact that two polarons with the same spin cannot occupy the same $k=0$ state. The picture changes at larger momenta, where both bands have similar weight, although the sharp peaks in $A_{\downarrow}$ are higher than the broadened features in $A^{\uparrow}$.

With increasing el-ph coupling, the low-energy bipolaron band becomes even narrower until it is virtually flat at $\lambda=1.5$ [Fig. 1(c)]. Here, the two conditions for a small bipolaron (Sec. II) are identical to $\lambda>0.5$. Consequently, finite-size effects are very small in Figs. 1(b)–1(d), as confirmed by the excellent agreement of the CPT data with the results for $E^{\uparrow\downarrow}(k)$. The reduction in bandwidth with increasing $\lambda$ is accompanied by a loss of spectral weight. For $k=0$, the latter decreases from the value 0.68 at $\lambda=0.5$ given above to about 0.10 at $\lambda=2.0$. Both the narrowing and the loss of weight indicate a significant increase of the effective bipolaron mass.

While the polaron band lies relatively close to the bipolaron band at $\lambda=0.5$ [Fig. 1(a)], the increase of the coupling leads to a clear separation, and to a downward shift of both bands proportional to the polaron binding energy $E_{\mathrm{P}}$. In the antiadiabatic strong-coupling regime of Fig. 1(d), the energy gap between the two bands is well described by the atomic-limit value $2E_{\mathrm{P}}=8t$. Similar to $\lambda=0.5$, the two-polaron band dispersion $E^{\uparrow}(0)+E^{\uparrow}(k)$ agrees well with the polaron band in the spectra, with some differences being visible near $k=0$. Interestingly, in Fig. 1(c), there is a mixing of the bipolaron state with one phonon excited, which lies an energy $\omega=4t$ above the lowest band, and the two-polaron excitation.

The polaron band also narrows with increasing el-ph coupling (see also I). However, the effect is much smaller than for the bipolaron band. Additionally, the spectral weight of the $k=0$ polaron peak in $A_{\uparrow}$ increases from about 0.20 at $\lambda=0.5$ to about 0.32 at $\lambda=2.0$. This may be explained by the fact that for weak coupling [Fig. 1(a)], some of the weight of the polaron state is contained in the large low-energy feature. Calculations for a single electron and the same parameters show that the spectral weight of the polaron at $k=0$ decreases from about 0.86 ($\lambda=0.5$) to about 0.52 ($\lambda=2.0$). Since the spectral weight is, to a very good approximation, equal to the inverse of the effective mass of the Holstein polaron,[45] these results indicate that the polaron mass does not increase at the same rate as the bipolaron mass with increasing coupling, as reflected by the corresponding changes in bandwidth in Fig. 1. Finally, we also find a comparable reduction of spectral weight for the two-polaron band in $A_{\downarrow}$ from about 0.08 ($\lambda=0.5$) to about 0.04 ($\lambda=2.0$) at $k=0$.

To conclude the discussion of the case $\overline{\omega}=4$, we would like to underline the enormous advantage of CPT in the strong-coupling regime. It permits us to perform calculations on a very small cluster ($N=4$)—sufficient to obtain well-converged results—but still yields the spectral function at any desired $k$.

### B. Intermediate phonon frequency

In the preceding section, we have investigated in detail the signatures of polaron and bipolaron states in the one-particle spectrum for $\overline{\omega}=4$. Owing to the large energy of phonon excitations, most of the spectral weight resides in the corresponding bands, allowing a fairly easy identification. We now consider the case $\overline{\omega}=1$, which turns out to be more difficult to study numerically and to interpret. Nevertheless, work in the regime $\overline{\omega}\leqslant 1$ is highly desirable to understand many interesting strongly correlated systems such as, e.g., the manganites. Although the latter are usually characterized

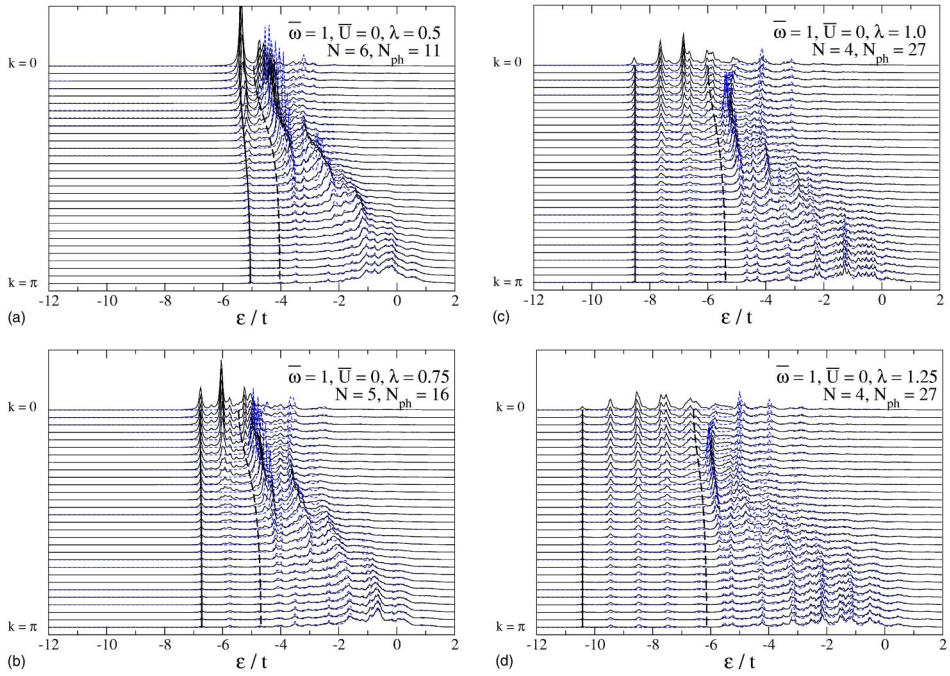


FIG. 3. (Color online) Spectral functions $A_\uparrow(k,\varepsilon)$ (solid lines) and $A_\downarrow(k,\varepsilon)$ (dashed lines) calculated with CPT for different values of the el-ph coupling λ, using $\eta=0.05t$. All other parameters as indicated in the figures. The truncation errors are $\Delta<$ (a) $9.1\times10^{-5}$, (b) $9.0\times10^{-5}$, (c) $1.2\times10^{-7}$, (d) $2.4\times10^{-6}$. The vertical lines correspond to variational diagonalization results for the polaron and bipolaron band dispersions $E^\uparrow(0)+E^\uparrow(k)$ (dashed) and $E^{\uparrow\downarrow}(k)$ (solid), respectively (Ref. 44).

by $\omega\ll t$, quantum effects are already visible for $\omega=t$. As a consequence, previous authors[4,17,34–36,38] have often focused on this case, which is numerically much easier to tackle than the region $\bar{\omega}\ll1$. The case $\bar{\omega}\ll1$ has been considered, e.g., by Wellein *et al.*[30] and Weiße *et al.*[32,41] While the discussion for $\bar{\omega}=4$ was restricted to $\bar{U}=0$, here we shall also take into account a finite Coulomb repulsion.

### *1.* $\bar{U}=0$

Since converged results for $\bar{\omega}=1$ require more phonon states than for $\bar{\omega}=4$, we have slightly reduced the cluster sizes in our calculations. Consequently, finite-size effects are larger, as discussed below. Moreover, we are not able to reach the strong-coupling regime but instead restrict the range of λ to 0.5-1.25.

Figure 3 contains the one-particle spectra for $\bar{U}=0$. In principle, for $\lambda=0.5$, the results look quite similar to Fig. 3(a). However, the spectral weight of the two coherent bands is much smaller, as a consequence of the increased importance of incoherent excitations for $\bar{\omega}=1$. In particular, the weight of the latter is strongly enhanced at large $k$, so that the bands are no longer easy to identify. Therefore, and because of the strong mixing of the bands with coherent and incoherent excitations, it becomes difficult to accurately determine the spectral weight by integration over the CPT spectra.

We see from Fig. 3 that the bipolaron bandwidth is much smaller for $\bar{\omega}=1(W'/W\approx0.1)$ than for $\bar{\omega}=4$ [Fig. 1(a)], despite the fact that the value of λ is the same in both cases. Hence, the effect of el-ph interaction on the bipolaron mass is much more pronounced in or near the adiabatic regime due to the larger mass of the oscillators.

In principle, the spectrum also contains coherent excited states which are separated from the lowest-energy band by less than the phonon energy $\omega$. However, owing to the rather complex structure of the spectrum in the two-electron case, they are difficult to distinguish from the other contributions. A direct calculation of excited states in the Holstein model with one electron has recently been presented by Barišić.[46] Finally, the relation between $A_\downarrow$ and $A_\uparrow$ is very similar to $\bar{\omega}=4$.

As we increase the el-ph coupling, the bipolaron dispersion collapses to an extremely narrow band [Fig. 3(b)]. This cross over is again associated with a significant loss of spectral weight. At $k=0$, for example, we find a reduction from about 0.50 at $\lambda=0.5$ to about 0.14 at $\lambda=0.75$. Increasing λ further to 1.25, we finally arrive at a bipolaron band with $W'/W\approx10^{-4}$ and a spectral weight of less than 0.03 at $k=0$. Similar to Fig. 1(d), the spectrum displays several bands equally spaced by $\omega$, which belong to states with one or more phonons excited. Moreover, the polaron and bipolaron bands are well separated, and the incoherent contributions dominate at large $k$.

The agreement between the bipolaron band dispersion and $E^{\uparrow\downarrow}(k)$ in Fig. 3 is again very good. Similar to $\bar{\omega}=4$, the condition for a small bipolaron is given by $\lambda>0.5$, so that CPT yields very accurate results. In contrast, the two-polaron energy $E^\uparrow(0)+E^\uparrow(k)$ fits less well to the corresponding bands in the spectral function. We attribute this difference to the antiadiabatic regime (Fig. 1 to the stronger retardation effects for $\bar{\omega}=1$. As a consequence, the polaron state is more extended below the small-polaron cross over occurring at $\lambda=1$ (see, e.g., I), leading to a stronger residual interaction on

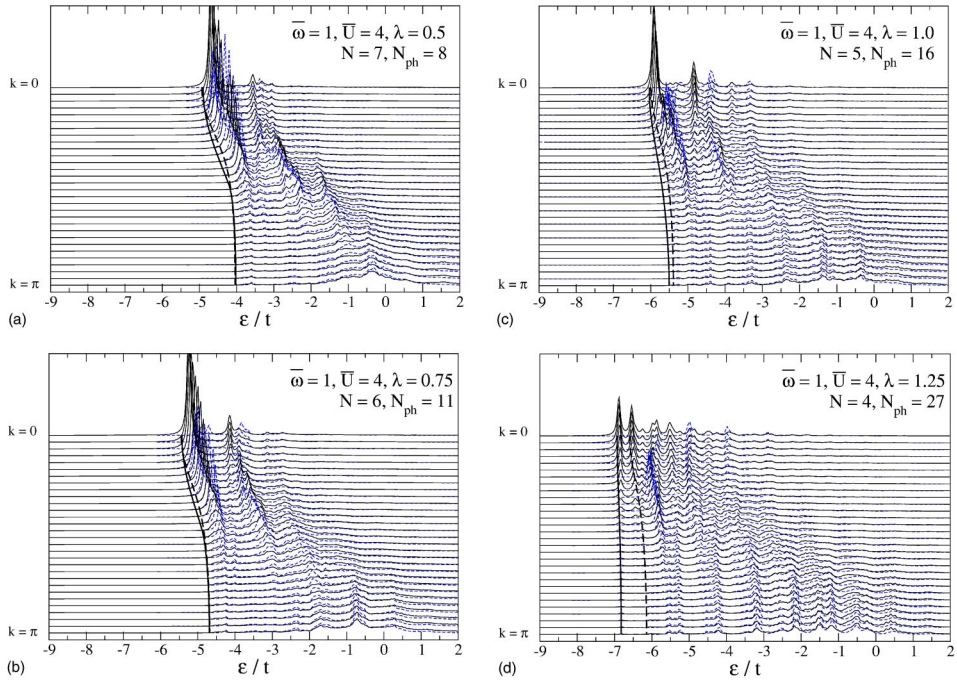


FIG. 4. (Color online) Spectral functions $A_{\uparrow}(k,\epsilon)$ (solid lines) and $A_{\downarrow}(k,\epsilon)$ (dashed lines) calculated with CPT for different values of the el-ph coupling λ, using $\eta=0.05t$. All other parameters as indicated in the figures. The truncation errors are $\Delta<$ (a) $3.3\times10^{-5}$, (b) $2.0\times10^{-5}$, (c) $9.9\times10^{-6}$, (d) $6.7\times10^{-7}$. The vertical lines correspond to variational diagonalization results for the polaron and bipolaron band dispersions $E^{\uparrow}(0)+E^{\uparrow}(k)$ (dashed) and $E^{\uparrow\downarrow}(k)$ (solid), respectively (Ref. 44).

a finite cluster, which also manifests itself in the CPT results. In contrast, for $\bar{\omega}=4$, the lattice distortions around the electrons are very localized, and the two polarons are almost independent. Above $\lambda=1$, i.e., in the small-polaron regime, the two-polaron dispersion for $\bar{\omega}=1$ again follows closely a two-polaron-like feature in the spectrum [Figs. 3(c) and 3(d)].

### 2. $\bar{U}=4$

So far, we have only presented results for $\bar{U}=0$, for which a bipolaron state is always favored. However, in materials such as the cuprates or the manganites, strong local correlations hinder the carriers from forming on-site bipolarons even for strong el-ph coupling. To model such effects, we therefore consider here a finite value of the el-el repulsion $\bar{U}=4$.

In the case of two electrons with opposite spin, the Lanczos results for the cluster Green function converge faster as a function of $N_{\mathrm{ph}}$ for $\bar{U}>0$ compared to $\bar{U}=0$ as a result of the reduced effective el-el interaction. This is fortunate, since it allows us to use slightly larger clusters, thereby partly compensating for the increased finite-size effects due to the spatially more extended ground state in the weak-coupling regime.

From the general discussion in Sec. II, we expect the ground state to consist of two weakly bound polarons for $2E_{\mathrm{P}}<U$, and a crossover to a bipolaron state at a critical value of the el-ph interaction λ. In the antiadiabatic limit, the latter is determined by $2E_{\mathrm{P}}=U$ (i.e., $\lambda=1$ for the case considered here) for weak coupling, and by $4E_{\mathrm{P}}=U$ for strong coupling.

In Fig. 4, we present the results for the spectral function, again for $\lambda=0.5$–1.25. For weak coupling $\lambda=0.5$ [Fig. 4(a)], the most striking difference from the $\bar{U}=0$ case discussed above is the fact that there appears only one band at low energies. Together with the incoherent contributions, and taking into account the doubling of the number of carriers leading to a shift of energies, the spectrum bears a close resemblance to that of a single polaron with the same parameters (Fig. 3 of I). This is also underlined by the polaron and bipolaron band dispersions shown in Fig. 4(a), which are almost identical throughout the Brillouin zone, and lie just below the corresponding band in the spectral function. In particular, the band displays the typical flattening at large $k$, where the low-energy excitations have mostly phononic character. Furthermore, owing to the finite on-site repulsion, the low-energy band in $A_{\downarrow}$ is very similar to that in $A_{\uparrow}$ since, for finite $\bar{U}$ and weak el-ph coupling, the singlet ground state consists of two weakly bound polarons. Consequently, the singlet and triplet states have comparable energies, although the spectral weight in $A_{\downarrow}$ is again very small near $k=0$.

For $\lambda=0.75$ [Fig. 4(b)], the ground state of the system is still given by two polarons, and the spectrum is almost indistinguishable from $\lambda=0.5$. In the present case, the condition for the existence of an intersite bipolaron is expected to lie between the weak- and strong-coupling results $U<2E_{\mathrm{P}}$ and $U<4E_{\mathrm{P}}$.[17] However, owing to its small binding energy, the intersite state is difficult to distinguish from the two-polaron state in the spectral function.

At $\lambda=1.0$ [Fig. 4(c)], the band in $A_{\uparrow}$ begins to split. Although the energy difference between the polaron and bipolaron band dispersions is still relatively small near $k=0$, an

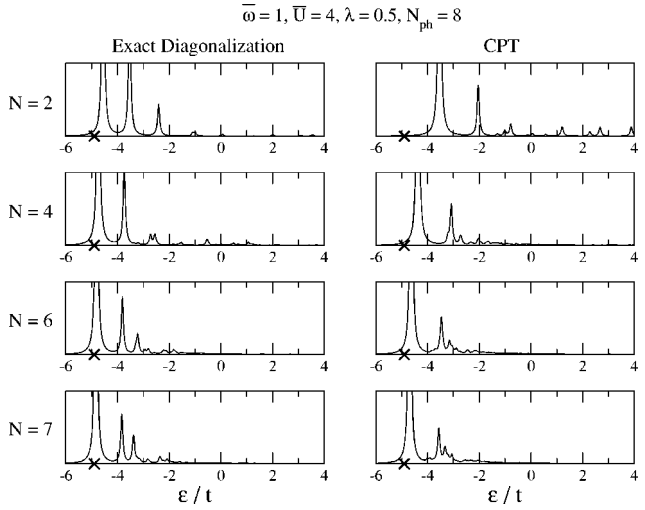


FIG. 5. Comparison of the spectral function $A_{\uparrow}(0,\epsilon)$ calculated with ED and CPT, respectively, for different cluster sizes $N$, using $\eta=0.05t$. The crosses correspond to the VDM result for the bipolaron energy $E^{\uparrow\downarrow}(0)$ (Ref. 44).

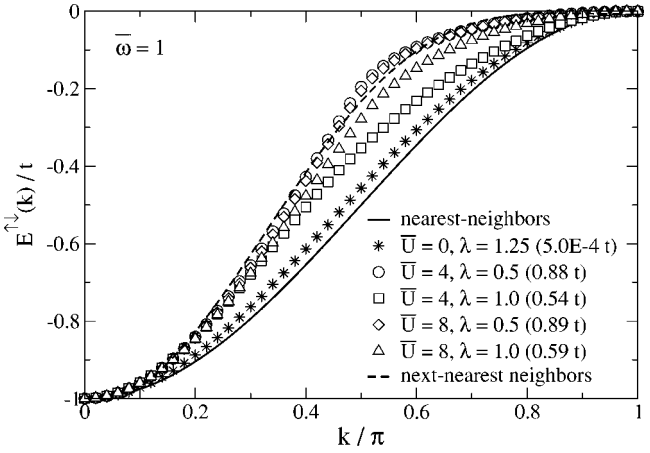


FIG. 6. Bipolaron dispersion $E^{\uparrow\downarrow}(k)$ as a function of the wave vector $k$ (Ref. 44). Also shown is the bare tight-binding dispersion for nearest-neighbor hopping, and a fit to the results for $\bar{U}=4$, $\lambda=0.5$ using a dispersion for nearest- and next-nearest-neighbor hopping (see text). All curves have been scaled to the interval $[-1,0]$, with the actual bandwidths given in the legend.

excitation gap clearly emerges at larger $k$. Finally, at $\lambda=1.25$, two distinct bands with similar spectral weight have formed, which agree very well with $E^{\uparrow\downarrow}(k)$ and $E^{\uparrow}(0)+E^{\uparrow}(k)$, respectively. Interestingly, the band in the triplet spectral function $A_{\downarrow}$ lies noticeably higher than the polaron band in $A_{\uparrow}$. Thus, for the parameters considered here, two polarons of opposite spin can lower their total energy by occupying the same lattice site, which is just the mechanism behind bipolaron formation.

The abovementioned discrepancies between the bipolaron band dispersion $E^{\uparrow\downarrow}(k)$ obtained by Shawish and the band in $A_{\uparrow}$ are a result of finite-size effects in the CPT calculations. The latter become smaller with increasing coupling $\lambda$ together with the size of the bipolaron, and for $\lambda=1.25$ we find a very good agreement [Fig. 4(d)]. To illustrate this point, we compare in Fig. 5 the spectral function $A_{\uparrow}$ at $k=0$, $\lambda=0.5$, and for different cluster sizes $N$, calculated using ED with periodic boundary conditions (left column) and CPT (right column), respectively. The results reveal that for weak coupling and intermediate $\bar{U}$, ED is superior to CPT concerning the convergence of the peak positions with respect to system size. This is not surprising as CPT is based on a strong-coupling expansion in the hopping term.[7] Here, the el-el and el-ph interactions are both of about the same magnitude as the hopping, so that the method does not work as well as for $\bar{U}=0$.

For $\bar{U}>0$, finite-size effects in both CPT and ED are larger due to the extended bipolaron state which exists for weak coupling. Similar to the one-electron case discussed in I, deviations from the exact results due to the finite cluster size are usually smallest for $k=0$, while they become larger with increasing $k$. Although in Fig. 5 the positions of the peaks in the CPT spectral function are slightly less accurate than in the case of ED, the weights of the excited states resemble more closely the results in the thermodynamic limit.

Finally, for $\bar{U}>4$, the crossover to a small bipolaron occurs at even larger values of $\lambda$. Apart from the change of the critical coupling, the physics is not altered significantly. Therefore, we have restricted our discussion of the spectral function to $\bar{U}\leqslant 4$, but some results for the bipolaron band dispersion at $\bar{U}=8$ will be presented below.

### *3. Bipolaron band dispersion*

The bipolaron band dispersion $E^{\uparrow\downarrow}(k)$ has been calculated before by Wellein *et al.*[30] and Weiße *et al.*[32,41] for small phonon frequencies $\bar{\omega}=0.4$ and $\bar{\omega}=0.5$, respectively. Remarkably, for parameters $\bar{U}>0$ and $\lambda>0$ such that the effective interaction $U_{\mathrm{eff}}=0$ [Eq. (3)], they found a renormalized, free-particle dispersion relation.[32,41] In this section, we wish to extend these considerations to the case $\bar{\omega}=1$, and to infinite systems. While the narrowing effect due to el-ph interaction has been discussed above, here we focus on the form of the band.

Owing to the limited energy resolution and finite-size effects in the CPT results shown above, we use the more accurate data from the VDM. In Fig. 6, we show Shawish's[44] results for the bipolaron energy as a function of $k$, for different values of $\bar{U}$ and $\lambda$. To permit a direct comparison, we have scaled all curves to the interval $[-1,0]$, with the actual bandwidths given in the legend.

We begin with the regime of a strongly bound small bipolaron. To this end we consider the case $\bar{U}=0$ and $\lambda=1.25$. The corresponding band resembles quite closely a cosine dispersion, with some deviations being visible around $k=\pi/2$. A different behavior is found for finite $\bar{U}=4$, as well as weak coupling $\lambda=0.5$. For these parameters, which favor a ground state with two polarons [see Fig. 4(c)], the form of the band is remarkably different from a simple tight-binding dispersion for nearest-neighbor hopping. This is still true for $\lambda=1$, although a trend toward a cosine dispersion is visible. For even larger $\bar{U}=8$, the noncosinelike form persists even for $\lambda=1$.

It is worth mentioning the great similarity of the results for $\bar{U}=4$ and $\bar{U}=8$ in the weak-coupling regime, which fol-

lows from the fact that once the small (on-site) bipolaron state is energetically unfavorable for the two electrons due to the Coulomb repulsion, a further increase of the latter has very little effect. On top of that, the intersite bipolaron state which exists for $\bar{U}>0$ has a very small binding energy, so that the band dispersion is almost the same as that of two polarons.

To identify the origin of the deviations from a free-electron band, we also included in Fig. 6 a fit of a free-electron model with nearest- and next-nearest-neighbor hopping to the band for $\bar{U}=4$ and $\lambda=0.5$, which yields an amplitude $t' \approx 0.6t$ for two-site hopping processes. As proposed by Wellein *et al.*,[30] the importance of long-range hopping for the band dispersion of a single polaron may be due to a residual polaron-phonon interaction, with the phonons and the polaron residing on different sites. Since we find substantial deviations of the bipolaron band from a cosine dispersion only in the regime of two weakly bound polarons, it stands to reason to assume the same underlying mechanism.

Finally, we would like to comment on the fact that despite $U_{\mathrm{eff}}=0$ for $\bar{U}=4$ and $\lambda=1$ in Fig. 6, we do not have a simple cosine band, in contrast to the findings of Wellein *et al.*[30] and Weiße *et al.*,[41] which have been attributed to the formation of an intersite bipolaron.[41] In contrast, here we observe non-cosinelike behavior even in the regime where an intersite state exists. These differences are expected to be a result of the larger value of the phonon frequency (here $\bar{\omega}=1$, while $\bar{\omega}=0.4$ and 0.5 in Refs. 30 and 41, respectively), leading to a noticeable reduction of retardation effects. Moreover, since the critical coupling $\lambda_c$ decreases as $\bar{\omega}\to 0$, the bipolaron is more strongly bound in the work of Refs. 30 and 41, thereby suppressing the abovementioned nonlocal phonon-polaron interaction. Further work along these lines is highly desirable to understand the dependence of the bipolaron band dispersion on the phonon frequency in the regime $\bar{\omega}\leqslant 1$.

## V. CONCLUSIONS

We have presented a detailed study of the one-electron spectral function of the Holstein-Hubbard model with two electrons of either the same or opposite spin. The method employed here is cluster perturbation theory together with the Lanczos method, which represents a versatile and fast approach.

As a function of the electron-phonon and electron-electron interaction strength, polaron and bipolaron states manifest themselves as quasiparticle bands, and results have been compared to accurate data for the bipolaron energy dispersion. For weak coupling and/or intermediate to strong Hubbard repulsion, finite-size effects are visible, but are much smaller than in previous work restricted to small clusters. The major advantage of the present method is that the spectrum can be obtained at any point in $\boldsymbol{k}$ space, even when using clusters with only a few lattice sites for which enough phonon states can be kept in the calculation. This has allowed us to investigate the dispersion and the spectral weight of the quasiparticle features throughout the Brillouin zone. The results and their dependence on the model parameters have been discussed, and a perfect agreement has been found with the physical picture of the Holstein-Hubbard bipolaron emerging from previous work. A comparison of the bipolaron dispersion with a simple tight-binding band has revealed an important contribution from next-nearest-neighbor hopping processes in the regime of a weakly bound state.

Finally, the adiabatic regime of small phonon frequencies, characteristic of many real materials, remains an interesting and demanding open issue for future work.

## ACKNOWLEDGMENTS

This work has been supported by the Austrian Science Fund (FWF), Project No. P15834. M.H. and M.A. are grateful to DOC (the Doctoral Scholarship Program of the Austrian Academy of Sciences). We are indebted to David M. Eagles for stimulating correspondence, and to Samir El Shawish for useful discussions, as well as for providing us with previously unpublished data. Finally, we would like to thank Holger Fehske for making valuable comments on the manuscript.

*Electronic address: hohenadler@itp.tugraz.at

[1] *Lattice Effects in High Temperature Superconductors*, edited by Y. Bar-Yam, J. Mustre de Leon, and A. R. Bishop (World Scientific, Singapore, 1992).
[2] D. M. Edwards, Adv. Phys. **51**, 1259 (2002).
[3] M. Hohenadler, M. Aichhorn, and W. von der Linden, Phys. Rev. B **68**, 184304 (2003).
[4] J. Ranninger and U. Thibblin, Phys. Rev. B **45**, 7730 (1992).
[5] E. V. L. de Mello and J. Ranninger, Phys. Rev. B **55**, 14 872 (1997).
[6] E. V. L. de Mello and J. Ranninger, Phys. Rev. B **58**, 9098 (1998).
[7] D. Sénéchal, D. Perez, and M. Pioro-Ladrière, Phys. Rev. Lett. **84**, 522 (2000).
[8] D. Sénéchal, D. Perez, and D. Plouffe, Phys. Rev. B **66**, 075129 (2002).
[9] M. G. Zacher, R. Eder, E. Arrigoni, and W. Hanke, Phys. Rev. Lett. **85**, 2585 (2000).
[10] M. G. Zacher, R. Eder, E. Arrigoni, and W. Hanke, Phys. Rev. B **65**, 045109 (2002).
[11] C. Dahnken, E. Arrigoni, and W. Hanke, J. Low Temp. Phys. **126**, 949 (2002).
[12] D. Sénéchal and A. Tremblay, Phys. Rev. Lett. **92**, 126401 (2004).
[13] C. Dahnken, M. Aichhorn, W. Hanke, E. Arrigoni, and M. Potthoff, Phys. Rev. B **70**, 245110 (2004).
[14] M. Aichhorn, H. G. Evertz, W. von der Linden, and M. Potthoff, cond-mat/0402580 (unpublished).
[15] T. Maier, M. Jarrell, T. Pruschke, and M. Hettler, cond-mat/0404055 (unpublished).

[16] J. P. Hague, J. Phys.: Condens. Matter **15**, 2535 (2003).
[17] J. Bonča, T. Katrašnik, and S. A. Trugman, Phys. Rev. Lett. **84**, 3153 (2000).
[18] I. G. Lang and Y. A. Firsov, Zh. Eksp. Teor. Fiz. **43**, 1843 (1962) [Sov. Phys. JETP **16**, 1301 (1962)].
[19] H. Fehske, G. Wellein, G. Hager, A. Weiße, and A. R. Bishop, Phys. Rev. B **69**, 165115 (2004).
[20] A. S. Alexandrov and N. Mott, *Polarons & Bipolarons* (World Scientific, Singapore, 1995).
[21] G. D. Mahan, *Many-Particle Physics*, 2nd ed. (Plenum Press, New York, 1990).
[22] M. H. Cohen, E. N. Economou, and C. M. Soukoulis, Phys. Rev. B **29**, 4496 (1984).
[23] D. Emin, J. Ye, and C. L. Beckel, Phys. Rev. B **46**, 10 710 (1992).
[24] A. La Magna and R. Pucci, Phys. Rev. B **55**, 14 886 (1997).
[25] L. Proville and S. Aubry, Physica D **113**, 307 (1998).
[26] L. Proville and S. Aubry, Eur. Phys. J. B **11**, 41 (1999).
[27] L. Proville and S. Aubry, Eur. Phys. J. B **15**, 405 (2000).
[28] G. De Filippis, V. Cataudella, G. Iadonisi, V. Marigliano Ramaglia, C. A. Perroni, and F. Ventriglia, Phys. Rev. B **64**, 155105 (2001).
[29] F. Marsiglio, Physica C **244**, 21 (1995).
[30] G. Wellein, H. Röder, and H. Fehske, Phys. Rev. B **53**, 9666 (1996).
[31] H. Fehske, H. Röder, G. Wellein, and A. Mistriotis, Phys. Rev. B **51**, 16 582 (1995).
[32] A. Weiße, H. Fehske, G. Wellein, and A. R. Bishop, Phys. Rev. B **62**, R747 (2000).
[33] S. El Shawish, J. Bonča, L. C. Ku, and S. A. Trugman, Phys. Rev. B **67**, 014301 (2003).
[34] C. Zhang, E. Jeckelmann, and S. R. White, Phys. Rev. B **60**, 14 092 (1999).
[35] H. De Raedt and A. Lagendijk, Z. Phys. B: Condens. Matter **65**, 43 (1986).
[36] A. Macridin, G. A. Sawatzky, and M. Jarrell, Phys. Rev. B **69**, 245111 (2004).
[37] M. Hohenadler and W. von der Linden, cond-mat/0409573 (unpublished).
[38] J. Bonča and S. A. Trugman, Phys. Rev. B **64**, 094507 (2001).
[39] M. Hohenadler, H. G. Evertz, and W. von der Linden, Phys. Rev. B **69**, 024301 (2004).
[40] B. K. Chakraverty, J. Ranninger, and D. Feinberg, Phys. Rev. Lett. **81**, 433 (1998).
[41] A. Weiße, G. Wellein, and H. Fehske, in *High Performance Computing in Science and Engineering '01*, edited by E. Krause and W. Jäger (Springer-Verlag, Heidelberg, 2002), p. 131.
[42] J. K. Cullum and R. A. Willoughby, *Lanczos Algorithms for Large Symmetric Eigenvalue Computations* (Birkhäuser, Boston, 1985), Vols. I and II.
[43] G. Hager, E. Jeckelmann, H. Fehske, and G. Wellein, J. Comput. Phys. **194**, 795 (2004).
[44] S. El Shawish (private communication).
[45] H. Fehske, J. Loos, and G. Wellein, Phys. Rev. B **61**, 8016 (2000).
[46] O. S. Barišić, Phys. Rev. B **69**, 064302 (2004).